Science of the Total Environment 1029 (2026) 181735

Contents lists available at ScienceDirect

Science of the Total Environment

journal homepage: www.elsevier.com/locate/scitotenv

Cutaneous penetration and permeation of tritiated particles: Experimental evidence from the TITANS EU project

Greta Camilla Magnano [a,b,*], Giovanna Marussi [a], Matteo Crosera [a], Veronique Malard [c], Mickael Payet [d], Olivier Debellemanière [d], Stefano Covelli [e], Daniele Karlicek [e], Gianpiero Adami [a], Nicola Zingaretti [f], Marcella Mauro [b], Elena Pavoni [e], Francesca Larese Filon [b,**]

[a] Department of Chemical and Pharmaceutical Sciences, University of Trieste, Italy
[b] Clinical Unit of Occupational Medicine, University of Trieste, Italy
[c] Aix Marseille Univ, CEA, CNRS, BIAM, IPM, Saint Paul-Lez-Durance, F-13108, France
[d] CEA, IRFM, F-13108, Saint-Paul-lez-Durance, France
[e] Department of Mathematics, Informatics and Geosciences, University of Trieste, Via E. Weiss 2, 34128, Trieste, Italy
[f] Clinic of Plastic and Reconstructive Surgery, Academic Hospital of Udine, Department of Medicine (DMED), University of Udine, Italy

HIGHLIGHTS

- Tritiated stainless steel and cement particles were assessed for dermal permeation.
- *In vitro* tests with human skin simulated different environmental exposure conditions.
- Skin damage strongly enhanced tritium diffusion and retention within the tissue.
- Material-specific release mechanisms affected tritium mobility and skin transfer.
- Results support environmental risk assessment and worker protection strategies.

GRAPHICAL ABSTRACT

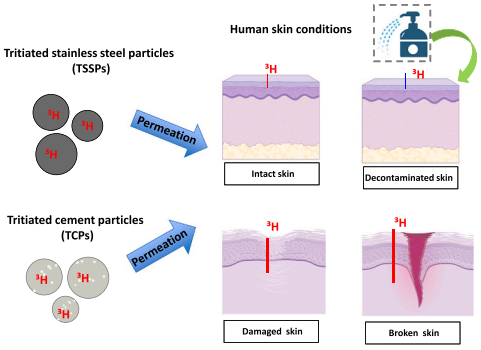

ARTICLE INFO

Keywords:
Tritium
Dermal absorption
Tritiated particles
Human skin
Franz cells
Skin decontamination

ABSTRACT

During nuclear facility decommissioning, the release of tritiated particulate matter from contaminated stainless steel and cement poses potential dermal exposure risks for workers and nearby environments. This study investigates the transdermal behavior of tritium (^{3}H) released from tritiated stainless steel (TSSPs) and cement particles (TCPs), two matrices differing in physicochemical composition and hydrogen-binding properties. Using *in vitro* Franz diffusion cells and excised human skin, ^{3}H permeation was evaluated under intact, damaged, abraded, and decontaminated skin conditions. Intact skin provided an effective barrier, whereas compromised epidermal integrity markedly enhanced ^{3}H diffusion and retention. Differences in ^{3}H release kinetics between particle types were associated with their surface characteristics and mechanisms of ^{3}H binding, solid-solution

* Correspondence to: G. Camilla Magnano, Department of Chemical and Pharmaceutical Sciences, University of Trieste, Italy.
** Corresponding author.
E-mail addresses: gmagnano@units.it (G.C. Magnano), larese@units.it (F. Larese Filon).

https://doi.org/10.1016/j.scitotenv.2026.181735
Received 14 October 2025; Received in revised form 20 March 2026; Accepted 22 March 2026
Available online 2 April 2026

entrapment in TSSPs *versus* isotopic exchange and surface adsorption in TCPs. The persistence of ^{3}H within partially damaged skin suggests potential formation of organically bound tritium (OBT), indicating localized and sustained radiobiological exposure. Importantly, simple water decontamination significantly reduced ^{3}H permeation, supporting its practical relevance in occupational dermal protection. These findings provide insight into the material interactions and dermal safety implications of tritiated particulates, contributing to risk assessment strategies in radiological and material exposure contexts.

1. Introduction

The dismantling and decommissioning of facilities contaminated with ^{3}H, whether from fusion, fission, or other industrial activities, inevitably generate tritiated particulate matter originating from structural materials such as stainless steel and cement. Cutting and mechanical operations can release these contaminated particles into the environment in the event of containment loss, raising potential health and safety concerns for workers and nearby populations. Despite the growing relevance of this issue, experimental data on the toxicological behavior and dermal absorption of radioactive particulates remain extremely limited (Ferreira et al., 2023). Although the dermal absorption of tritiated water (HTO) has been extensively studied since the 1960s, there is still a critical lack of knowledge regarding the percutaneous uptake of tritium bound to solid matrices, such as metallic and cementitious particles, materials highly representative of nuclear decommissioning scenarios. To date, no systematic evaluation of occupational skin exposure to tritiated particles has been reported, although the skin constitutes a major organ in direct contact with environmental and occupational contaminants. ^{3}H is a low-energy beta-emitting radioactive isotope of hydrogen with a half-life of approximately 12.3 years (Eyrolle et al., 2018). When incorporated into biological tissues, tritium decay can produce localized radiobiological effects (Dolin et al., 2025). Although tritium occurs naturally at atmospheric background levels (13 mBq/m^{3}) (Matsumoto et al., 2021), large-scale production occurs during fission and fusion processes. Once released, ^{3}Hrapidly oxidizes to form HTO, a highly mobile species capable of entering the body *via* inhalation, ingestion, or transdermal absorption (Pinson and Langham, 1957). Early human volunteer studies demonstrated that cutaneous exposure to HTO significantly contributes to systemic ^{3}H burden, with an impact comparable to inhalation (Osborne, 1966). Such findings also showed that multilayer protective garments and air-supplied masks can reduce dermal uptake by more than two orders of magnitude. Once absorbed, HTO distributes throughout body water compartments, exhibiting a biological half-life of about 10 days, while approximately 5–6% of absorbed ^{3}H becomes organically bound tritium (OBT), showing biphasic biological clearance (short-term of 40 days; long-term >1 year) (Kim et al., 2013; Paquet et al., 2016). Recent European research projects, including TRANSAT (https://transat-h2020.eu/) and TITANS (https://titans-project.eu/), have focused on the assessment of health and environmental implications associated with tritium-bearing particulate matter, particularly in terms of dispersion, exposure pathways, and toxicological effects, rather than attributing environmental risk directly to particulate matter *per se*. The TRANSAT project (Liger et al., 2018; Ferreira et al., 2023) investigated tritiated dust toxicity using *in vivo* models (Smith et al., 2022). Building upon these findings, the TITANS project extended the focus to cutaneous exposure, recognizing the importance of the skin as a potential route for internal contamination. In parallel, Larese Filon et al. (Filon et al., 2025) investigated the cutaneous absorption of non-radioactive metallic particles from hydrogenated stainless steel and cement, showing that metals such as Ni, Cr, and Co can permeate human skin and induce sensitization or allergic contact dermatitis, particularly in predisposed individuals. These observations highlight the importance of assessing dermal exposure pathways in addition to inhalation when evaluating nanotoxicological risks associated with engineered or contaminant particles. In the present study, we investigated tritiated materials, specifically TCPs and TSSPs. Using standardized *in vitro* Franz diffusion cell assays (OECD, 2004a; Hopf et al., 2020) and excised human skin, ^{3}H penetration and permeation were quantified under four experimental conditions: intact, damaged, abraded, and decontaminated skin. This experimental design aims to mimic realistic exposure scenarios and to assess the efficacy of decontamination procedures. Therefore, the central objective of this work is to determine whether and to what extent ^{3}H associated with TSSPs and TCPs can penetrate and permeate human skin, how different degrees of skin barrier impairment influence tritium penetration and cutaneous retention, and to what extent simple water decontamination can reduce the cutaneous tritium burden. Specifically, we address the following key scientific questions: (i) does ^{3}H bound to metallic and cementitious particles permeate through human skin; (ii) how do different levels of skin damage affect ^{3}H penetration and retention; and (iii) can simple decontamination procedures significantly mitigate dermal tritium exposure. To our knowledge, this is the first experimental study providing a quantitative assessment of ^{3}H skin absorption from contaminated metallic and cementitious nanostructured particles in human skin models. By focusing on dermal exposure pathways relevant to nuclear decommissioning, this work addresses a critical knowledge gap and contributes to improving radiological risk assessment and the development of effective protective and decontamination strategies for occupational settings.

2. Material and methods

2.1. Chemicals

Lactic acid (90% *v*/v) was obtained from Acros Organics (Belgium), while sodium hydrogen phosphate, potassium dihydrogen phosphate, sodium chloride, and urea were purchased from Carlo Erba (Italy). The physiological buffer solution was prepared by dissolving 2.38 g of Na_2HPO_4, 9.0 g of NaCl and 0.19 g of KH_2PO_4 in 1.0 L of ultrapure MilliQ water. The resulting solution exhibited a pH of approximately 7.35. A synthetic sweat formulation was prepared by dissolving lactic acid (0.1% *w/v*), urea (0.1% w/v) and sodium chloride (0.5% w/v) in MilliQ water. The pH of this solution was then adjusted to 4.5 by the dropwise addition of 1 N ammonium hydroxide, in order to mimic the typical acidity of human sweat.

2.2. Production of tritiated particles

The TSSP were purchased from Goodfellow (Goodfellow Cambridge Ltd., UK). They were studied in cold condition by Larese Filon et al. (Filon et al., 2025). In detail, these particles were hydrogenated to mimic the tritiation conditions. Median Aerodynamic diameter of TSSPs was 13.3 μm (monomodal distribution of particle size with a Geometric Standard Deviation of 4.7 μm). TCPs were obtained from Portland cement with an aerodynamic diameter of 4.9 μm (monomodal distribution of particle size with a Geometric Standard Deviation of 1.92 μm). The tritiation protocol was perfomed in the tritium lab in the CEA Paris-Saclay in three steps. A detailed description of the experimental apparatus, tritiation procedure, and analytical methods is provided in the Supplementary Materials. In the two first step, TSSPs were exposed at 450 °C for 2 h under H_2 (99.9%) at a pressure of $1.2 \pm 0.05 \times 10^{5}$ Pa and respectively 2 h at 450 °C under H_2 at $1.4 \pm 0.05 \times 10^{5}$ Pa. The third step was realized at 450 °C and $1.0 \pm 0.05 \times 10^{5}$ Pa either with H_2

leading to HSSPs or with T_2 leading to TSSPs. Once tritiation was complete, a final phase was performed to remove labile ^3H, defined as the fraction of ^3H weakly adsorbed on the particle surface or trapped in easily exchangeable forms. This step did not affect the structurally incorporated ^3H, which determines the final specific activity of the labeled powders. Degassing was carried out in air-flow using a bubbler-based apparatus (MARC 7000 from SDEC France), where gaseous ^3H (T_2 or HT) released from the sample was trapped in bottles containing H_2O (within HT species converted to HTO in the presence of a catalyst). The resulting HTO was collected and quantified *via* liquid scintillation counting (LSC) (Tri-Carb 2910TR analyzer from Perkin Elmer). The duration of the degassing step was material-dependent. For cement particles, equilibrium conditions (degassing plateau) were typically reached after 20–30 days, while for stainless steel powders, the process required approximately 10–15 days. The plateau confirmed the removal of the labile tritium fraction and the stabilization of the specific ^3H activity within the particles.

2.3. Dissolution test of tritiated particles

To evaluate the content of ^3H dissolved from TCPs and TSSPs, dissolution studies were conducted using synthetic sweat solutions. In brief, TCPs and TSSPs were immersed in 10 mL of synthetic sweat adjusted to pH 4.5. Over time, the release of ^3H into the solution was monitored using LSC, as detailed in Section 2.8. At predetermined intervals (0, 0.5,1,2,6 and 8 h), 0.5 mL samples were collected from the test medium, diluted 1:20 with Milli-Q water, and subsequently analyzed by LSC. To maintain the testing conditions, an equal volume of fresh synthetic sweat was replaced at each time point. All experiments were carried out in triplicate. ^3H release percentage was calculated as the ratio between the activity released at time (t) and the total activity initially present in the sample, multiplied by 100.

$$\text{Release}\,(\%) = \frac{\text{Activity release at time}\,(t)}{\text{Total activity initially present in the particle sample}}\,\text{x}\,100$$

This normalization was applied to allow a meaningful comparison of the release profiles between different particle types.

2.4. Preparation of tritiated particle suspensions in synthetic sweat

Two different suspensions containing tritiated particles were prepared as donor phases for the permeation assays. Specifically, two 1% *w/v* suspensions were freshly prepared in synthetic sweat: one containing TCPs and the other containing TSSPs. Due to the high sensitivity of the ^3H detection instrument, both suspensions were diluted to achieve a final ^3H activity of 37 and 84 Bq/mL, respectively. Then, 1.0 mL of each ^3H-labeled particle suspension was applied to the respective donor compartment.

2.5. Human skin specimens

Human abdominal skin specimens were obtained from surgical waste material, following ethical approval granted by the Ethical Committee of Trieste Hospital (authorization no. 236/2007). The tissue donors were both male and female, aged between 50 and 65 years. After excision, the subcutaneous adipose tissue was carefully removed using a scalpel. The skin samples were then stored at −25 °C for no longer than four months. Prior to use, the skin was thawed at room temperature and immersed in physiological saline solution to preserve hydration. A micrometer caliper (Mitutoyo) was employed to standardize the thickness of the skin to 1.05 ± 0.02 mm. The membranes were then cut into 4 cm^2 sections. To ensure barrier integrity, transepidermal water loss (TEWL) was measured using a vapometer (Delfin). Only samples with TEWL values below 10 $g{\cdot}m^{-2}{\cdot}h^{-1}$ were included in the study, as indicative of intact epidermal function, according to the literature (Guth et al., 2015).

2.6. Transdermal absorption assay tritiated particles

In accordance with OECD guidelines (OECD, 2004a), skin absorption assays were performed using Franz diffusion cells, as represented in Fig. 1.

Sections of human skin were mounted between the donor and receptor chambers, with an effective diffusion area of 3.14 cm^2. The receptor chamber was filled with 4.5 mL of physiological solution (composition described in Section 2.1) and continuously stirred with a magnetic stirrer. The system was maintained at a temperature of 32 ± 1 °C using a thermostated water bath. At the beginning of the experiment ($t = 0$), 1.0 mL of each ^3H labeled particle suspension, at defined activity levels, was applied to the skin surface. Aliquots of 0.5 mL were collected from the receptor solution at predetermined time points (0.5, 1, 2, 6, and 8 h) and replaced immediately with fresh solution to ensure sink conditions throughout the assay.

Four experimental conditions (intact, damaged, broken and decontaminated) were evaluated as follows:

Experiment 1. Intact skin. Skin samples were left unmodified to assess baseline permeation.

Experiment 2. Damaged skin. Superficial microlesions were created using a standard syringe needle (26 G, ~0.45 mm diameter), drawing five times in one direction and five times perpendicular, following the method described by Bronaugh and Steward (Bronaugh and Stewart, 1985). This procedure creates superficial microlesions suitable for permeation studies.

Experiment 3. Decontaminated skin. Here, 1.0 mL of tritiated particle suspension was applied to the center of the skin surface. After 15 min of exposure, the skin was decontaminated by sprinkling 3 mL of water as droplets onto the surface. Following a two-minute contact, the solution was removed, and residual tritiated particle suspensions were wiped off with a cotton swab soaked in the decontamination solution. After cleaning, 1.0 mL of synthetic sweat was added to the donor chamber. To assess the effect of decontamination, the permeation test was carried out over 8 h.

Experiment 4. Broken skin. A 5 mm longitudinal incision was made in the center of the exposed area using a scalpel to simulate a compromised barrier.

A total of four independent biological replicates were performed using skin samples from two donors, resulting in 16 samples per time point (80 independent analyzed cells). Procedural controls, including blank, were implemented to minimize variability. Uncertainty estimates

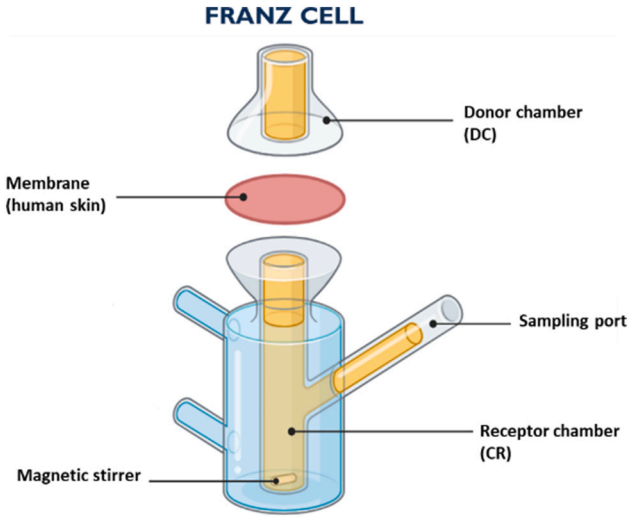

Fig. 1. Franz diffusion cell, modified by BioRender.

considered instrumental and biological variability.

2.7. Samples treatment

After 8 h (end of the experiment), the skin surface was rinsed three times with 1.0 mL of Milli-Q water to remove any residual material. Subsequently, the Franz diffusion cells were disassembled. The receptor fluid was collected for ^{3}H quantification. Each skin membrane was then transferred into a vial containing 20 mL of Milli-Q water and incubate for 1 h at room temperature (22–25 °C) to facilitate ^{3}H extraction. After this period, a 1.0 mL aliquot was withdrawn from the vial for ^{3}H tritium analysis.

2.8. Tritium quantification and data analysis

The analyses for the determination of ^{3}H activity in the samples were performed according to the procedures specified in (ISO, 2019) and (IAEA, 1998). To prepare the samples for counting, vials manufactured by ZINSSER ANALYTIC GMBH (model ZINSSER POLYVIALS®, item number: 307140, volume: 20 mL, material: HDPE 2) were used. Each vial was filled with a mixture of 10 g of sample and 10 g of Ultima Gold LLT scintillating liquid (manufactured by Revvity Health Sciences B.V.). The resulting mixture was shaken well and left to stand for 3 h (manufacturer's recommended time). The samples were then inserted into the LKB Wallac (now Revvity Health Sciences B.V.) "Low Level Scintillation Counter Quantulus 1220", and each sample was subjected, according to standardized procedures, to 8 counting cycles of 40 min each. Two very old water samples, taken from a well approximately 400 m deep and with zero ^{3}H activity (so called "dead" water), were used as background. This method takes into account a 10% error. Tritium is expressed in TU (Tritium Units), which is the value of the ratio of 1 ^{3}H atom to $10^{18}H$ atoms, a value corresponding to the concentration of the isotopes in ocean surface waters ($T/H = 1/10^{18}$). The historical unit of decay is the Curie, defined as the number of disintegrations per second due to one gram of $^{226}_{88}Ra$. The most widely used new unit of measurement is the Becquerel, which equals one disintegration per second. The well known conversions are:

(1) 1 Ci = 3.7 * 10^{10} Bq

(2) 1 nCu = 37 Bq

(3)1TU = 3.25 pCi L^{-1} = 0.118 Bq L^{-1}

The instrument allows the activity of a radionuclide to be determined by providing a parameter called CPM (Counts Per Minute) according to the frequency described as follows:

CPMs are the result of the transfer functions used to measure decay activity.

The following quantities were used: CPM (Counts Per Minute), DPM (Disintegrations Per Minute) where1DPM = 60 Bq and E (Efficiency) as follows:

(4) $E\,[\%] = \frac{Net\ Number\ of\ Counts\ Detected}{Number\ of\ Decay\ Events}\ x\ 100$

The Quantulus 1220 used in this work has an Efficiency of 55.1.

Knowing that 1 TU has an activity of 1.1813 * 10^{-4} Bq/g, the analyzed samples weighting 10 g, the CPM are:

(5) CPM = 1.1813 * 10^{-4} * 10 * 60 * E = 0.0709 * E

Therefore, knowing the number (n) of CPMs, the TU can determined as follows:

(6) $nTU = \frac{nCPM - Background}{0.0709 * E}$

Accordingly, the final value in Becquerel/g of each sample is then calculated.

2.9. Permeability calculation

The flux (J) was determined using Eq. (1):

$$J = \frac{dQ}{A*dt} \quad (1)$$

where dQ represents the cumulative amount of ^{3}H permeated through the membrane (in Bq), dt is the time interval (in hours), and A is the exposed membrane area (in cm^2). The flux was calculated as the slope of the cumulative permeation *versus* time curve during the steady-state period, which reflects the driving force for diffusion (*i.e.*, the concentration difference across the membrane).

The permeability coefficient (K_p, in cm/h) was calculated using the flux value (J, in Bq/cm^2/h) and the concentration of tritium in the donor solution (C_d, in Bq/cm^3), according to Eq. (2)

$$k_p = \frac{J}{C_d} \quad (2)$$

This approach allows for a reproducible quantification of ^{3}H permeation under controlled experimental conditions (receptor solution, temperature 32 °C).

2.10. Statistical analysis

The results are shown as (Bq/cm^2/h) corresponding to the amount of ^{3}H that permeated through skin per unit of skin surface in function of the time or as total skin content (% of applied ^{3}H), indicating the fraction of ^{3}H retained in the skin relative to the total applied. Due to the non-normal distribution of the data, non-parametric statistical analysis was performed. Differences between groups were assessed using the Wilcoxon rank-sum test. A *p*-value below 0.05 was considered statistically significant.

3. Results

3.1. Determination of the specific tritium activity in TSSPs and TCPs

TSSPs and TCPs were successfully prepared and their specific activities were determined by LSC. A total of 330 mg of TSSPx exhibited a specific activity of 0.9 ± 0.0 GBq/g, indicating efficient incorporation of ^{3}H within the metallic matrix. In comparison, 260 mg of TCP showed a lower specific activity of 0.1 ± 0.0 GBq/g. These differences are related to the thermally-activated diffusion process for TSSPs treated at 450 °C, but also likely due to the distinct physicochemical properties of the two materials, which influence ^{3}H diffusion and binding capacity. The specific activities obtained were considered suitable for use in subsequent permeation and decontamination experiments. All data are summarized

Table 1
Characteristics of the tritiated particles used in the study.

Particles	Amount ^{3}H particles (mg)	Specific activity [GBq/g]
Tritiated stainless steel (TSSPs)	330	0.9 ± 0.0
Tritiated cement particles (TCPs)	260	0.1 ± 0.0

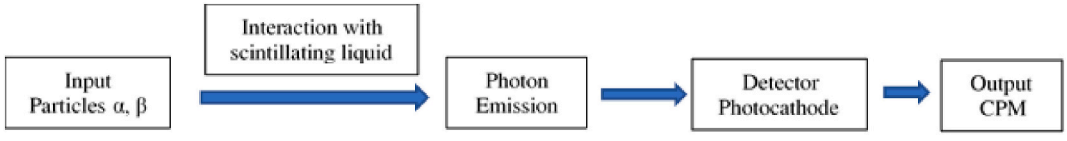

in Table 1.

3.2. Dissolution of tritiated particles in synthetic sweat

The dissolution profile of TSSPs and TCPs in synthetic sweat was evaluated over an 8-h period. As shown in Fig. 2, both particle types released ^{3}H into the medium in a time-dependent manner. ^{3}H release was expressed as percentage of release relative to the total ^{3}H content of each particle sample as reported in Section 2.3. At 8 h, TSSPs released 52 ± 5.7% of their total tritium content, while TCPs released 46 ± 2.9%. Both profiles showed good linearity over time, with correlation coefficients of $R^2 = 0.97$ for TSSPs and $R^2 = 0.87$ for TCPs, indicating similar overall release kinetics. These data suggest that, the relative dissolution behavior of the two particle types in synthetic sweat is broadly comparable.

3.3. Cumulative skin permeation of tritiated stainless steel particles under different skin conditions

The cumulative permeation profiles of TSSPs and TCPs across different human skin condition were shown in Figs. 3 and 4, respectively. In intact skin, the amount of ^{3}H measured in receptor fluid (RF) at 8 h was relatively lower for both particle types, with TCPs showing slightly higher values (0.3 ± 0.0% of applied dose) compared to TSSPs (0.2 ± 0.0% of applied dose) (Figs. 3A and 4A). This reflects the effective barrier function of the skin. Moreover, decontaminated skin consistently exhibited the lowest permeation values with both tritiated particles showing the same cumulative percentage (0.1 ± 0.0% of applied dose for TSSPs and 0.1 ± 0.0% for TCPs), confirming the effectiveness of water decontamination in reducing residual radioactive particle absorption. On the other hand, damaged skin exhibited higher levels of permeation, with a marked increase of ^{3}H over time for both particle types. Notably, after 8 h, the cumulative percentage of ^{3}H permeated from TSSPs and TCPs was similar reaching a value of 0.4 ± 0.1% of applied dose, highlighting the increased vulnerability of compromised skin barriers to facilitate particle penetration. Similarly, in broken skin (Figs. 3B and 4B), both particle types showed a drastically increased of ^{3}H permeation rate reaching values of 19 ± 2.4% of applied dose for TSSPs and 22 ± 2.6% of applied dose for TCPs. These higher permeation profiles from both tritiated particles reflect the severe disruption of the skin barrier and the associated elevated risk of particle permeation.

Furthermore, the flux (J), and apparent permeability coefficient (P_{app}) were also calculated and summarized in Table 2. For TCPs, ^{3}H permeation through intact skin was limited, with a flux of 3.2 ± 0.6 mBq/cm^2/h, and a P_{app} of 0.2 ± 0.0 cm/h. In damaged skin, all parameters increased, with J reaching 5.0 ± 1.2 mBq/cm^2/h and a value of P_{app} ranging around 0.3 ± 0.1 cm/h. Decontaminated skin showed a marked reduction in permeation values, with J decreasing to 0.4 ± 0.3 mBq/cm^2/h and a P_{app} value of 0.02 ± 0.0 cm/h. The highest permeation occurred in broken skin, where J increased sharply to 398 ± 49 mBq/cm^2/h and P_{app} exhibited a value of 23 ± 2.9 cm/h. A similar trend was observed for TSSPs, though the absolute values were generally higher than those measured for TCPs (Table 2). Indeed, in intact skin, the flux was 6.8 ± 1.3 mBq/cm^2/h, with a P_{app} of 0.2 ± 0.1 cm/h. These values increased in damaged skin to 9.9 ± 2.2 mBq/cm^2/h for flux value (J), and 0.2 ± 0.0 cm/h for P_{app}. However, decontamination skin significantly reduced permeation profile, with values of J ranging around 1.1 ± 0.6 mBq/cm^2/h, and P_{app} equal to 0.03 ± 0.0 cm/h. Similarly to the data observed for TCPs, TSSPs exhibited the highest levels of ^{3}H from TSSPs permeated with a flux value of 766 ± 100 mBq/cm^2/h and a P_{app} of 17 ± 2.3 cm/h in broken skin. Overall, these results confirm the critical role of skin integrity in modulating ^{3}H absorption. Broken skin markedly enhances permeation, whereas decontamination effectively reduces ^{3}H penetration to minimal levels. The two particle types show similar permeation profiles, indicating that both particles interact with the skin in comparable ways. Minor differences observed may reflect subtle variations in particle size, surface properties, or affinity for skin components, but statistical analysis did not reveal significant differences between the two materials under any skin condition. These findings highlight that skin condition is the primary factor governing tritium permeation, while particle type may modulate interactions with the skin to a minor extent.

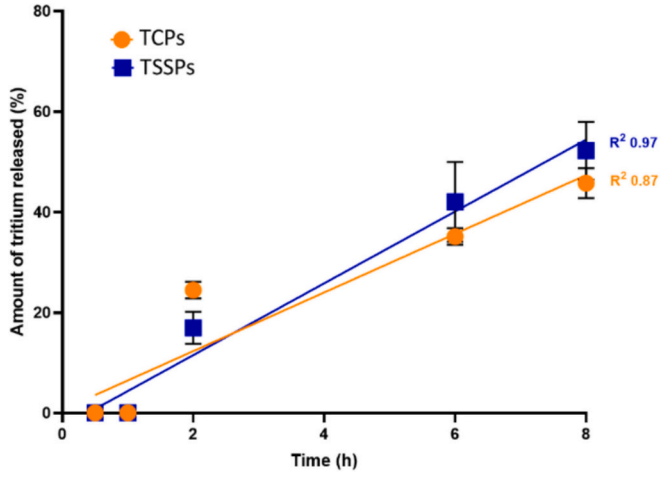

Fig. 2. Percentage amount of ^{3}H released from TSSPs and TCPs in synthetic sweat over 8 h. Data were expressed as (mean ± SD). ^{3}H release was expressed as percentage of release relative to the total ^{3}H content of each particle sample.

3.4. Skin retention of tritiated particles under different integrity conditions

The data presented in Table 3 and Fig. 5 showed the total skin retention of ^{3}H following exposure to TCPs and TSSPs under different skin conditions. For both particle types, damaged skin exhibits the highest levels of ^{3}H retention, with cumulative percentages of 90 ± 16% for TSSPs and 78 ± 22% for TCPs (Table 3; Fig. 5). This indicates that even partial disruption of the skin barrier significantly enhances the interaction of the radioactive material with the cutaneous tissue. Broken skin also shows high levels of ^{3}H retention (46 ± 12% for TSSPs and 57 ± 21% for TCPs), although these values were slightly lower than those observed in damaged skin. This may suggest that in fully compromised skin, part of the radioactive material penetrates more deeply reaching the receptor fluid, as observed in (Figs. 3A-B,4A-B and Table 2), leading to a lower residual accumulation in the skin tissue layer. However, in intact skin, the total amount of ^{3}H retained in the skin was substantially lower (4.2 ± 3.0% for TSSPs and 6.5 ± 4.3% for TCPs), confirming the effective barrier function of healthy skin in limiting particle absorption. Finally, decontaminated skin showed the lowest levels of ^{3}H retention in all conditions, (1.3 ± 0.5% for TSSPs and 1.5 ± 1.0% for TCPs), demonstrating the efficacy of water washing in removing radioactive particles from the skin surface and preventing further absorption. Overall, the results highlight the critical role of skin integrity in modulating the interaction with the radioactive particles, and underline the importance of immediate decontamination procedure in case of dermal exposure.

4. Discussion

This study provides a novel and detailed evaluation of ^{3}H permeation from TSSPs and TCPs through human skin using an *in vitro* Franz diffusion cell system. Although dermal exposure to ^{3}H has historically received less attention than inhalation or ingestion, our findings demonstrate that the skin can represent a relevant route of internal contamination, particularly when its barrier integrity is compromised. Quantitatively, ^{3}H retention and permeation through the skin remained

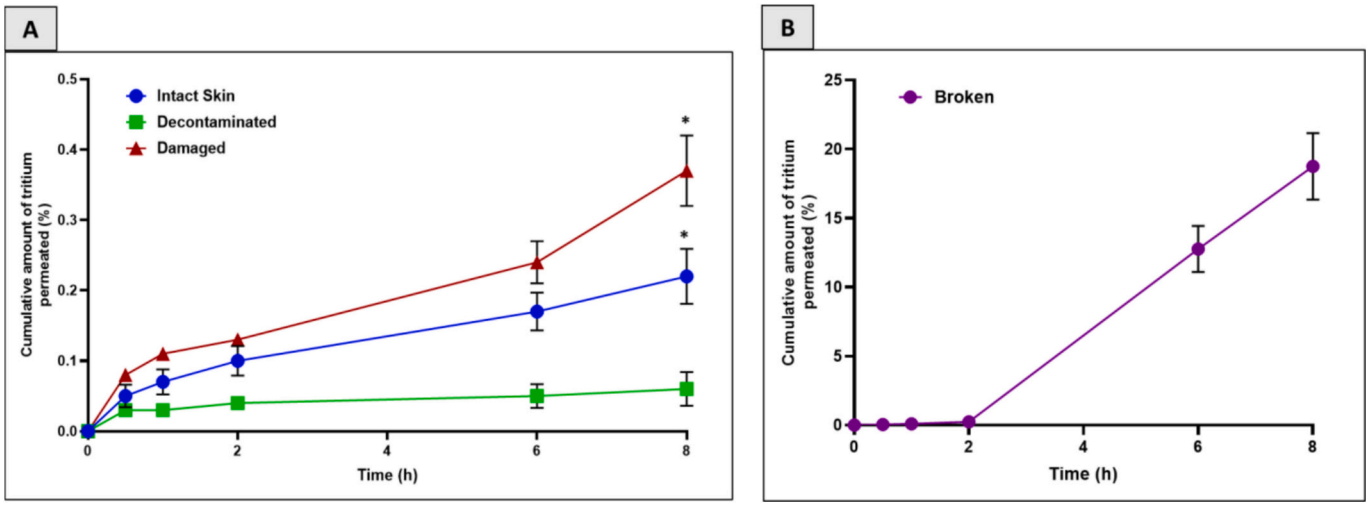

Fig. 3. (A) Permeation profile of TSSPs in intact, decontaminated and damaged skin. (B) Permeation profile of TSSPs in broken skin. Data are shown as mean ± SEM ($n = 4$).

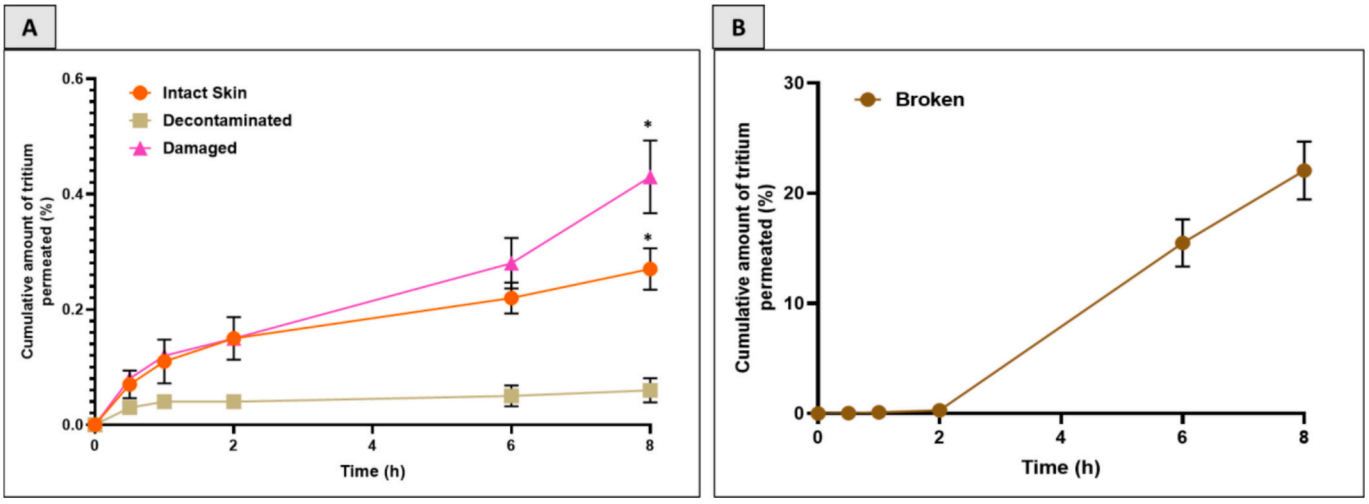

Fig. 4. (A) Permeation profile of TCPs in intact, decontaminated and damaged skin. (B) Permeation profile of TCPs in broken skin. Data are shown as mean ± SEM (n = 4).

below 1% of the applied dose in intact and decontaminated skin, whereas damaged and broken skin showed higher absorption, up to around 90% of the applied dose in the most extreme cases. These results provide a context for evaluating the relative contribution of dermal exposure to overall internal contamination and highlight the importance of barrier integrity in modulating ^{3}H uptake. To our knowledge, this is the first study to provide quantitative experimental data on the transdermal absorption of ^{3}H from particulate matrices, contributing to a largely unexplored aspect of occupational toxicology within the context of nuclear decommissioning and decontamination. Both tritiated materials released measurable amounts of ^{3}H into synthetic sweat, resulting in detectable skin permeation under all tested conditions. In intact skin, ^{3}H fluxes were minimal (< 10 mBq/cm^{2}/h Table 2), confirming the efficiency of the *stratum corneum* as a diffusion barrier. These observations are consistent with previous reports (Osborne, 1966) and OECD Guideline 428 for hydrophilic radiolabeled compounds (OECD, 2004b). Conversely, damaged and abraded skin showed up to 100-fold higher ^{3}H permeability, in agreement with previous literature studies indicating that even microstructural disruptions of the *stratum corneum* can significantly increase transdermal absorption (Kezic and Nielsen, 2009; Gattu and Maibach, 2010). These results have direct implications for workers involved in dismantling operations, where microabrasions, irritant dermatitis, and pressure-induced injuries are common and may increase susceptibility to dermal radionuclide absorption. The physicochemical characteristics of TSSPs and TCPs may influence both ^{3}H release and dermal permeation. Although minor differences were observed, with TSSPs showing a slightly higher release, both particle types exhibited a broadly comparable and time-dependent ^{3}H release profile in synthetic sweat (Fig. 2). This behavior can be attributed to metal hydride formation and the breakdown of the passive oxide layer typically present on stainless steel surfaces (Hollenberg et al., 1995), consistent with previous observations of hydride decomposition facilitating ^{3}H liberation from metallic matrices (Austin and Elleman, 1972; Matsuyama et al., 2011). In addition, TCPs displayed a slightly lower release profiles (Fig. 2), likely due to surface adsorption and isotopic exchange with structural water rather than bulk incorporation (Ono et al., 1995). Collectively, these findings indicate that the microscale structure and surface reactivity of metallic *versus* mineral matrices critically determine ^{3}H mobility and its subsequent interaction with biological barriers. Interestingly, both particle types exhibited increased ^{3}H retention in partially damaged skin compared to completely broken skin (Table 3, Fig. 5). This suggests that under moderate barrier

Table 2
J, P_{app} and ^3H concentration in RF at 8 h of TCPs and TSSPs under different skin conditions: intact; damaged; decontaminated and broken. Data are shown as mean ± SEM ($n = 4$). * Statistical differences between broken skin samples and the other skin conditions samples for TCPs; § statistically differences between decontaminated skin samples and the other skin conditions samples (intact-damaged) for TCPs; ¥ statistically differences between broken skin samples and the other skin conditions samples for TSSPs; † statistically differences between decontaminated skin samples and the other skin conditions samples (intact-damaged) for TSSPs.

Particles	Sample	J (mBq/cm²/h)	P_{app} (cm/h)	Tritium concentration in RF at 8 h (%)
Tritiated cement particles (TCPs)	Intact Skin	3.2 ± 0.6* §	0.2 ± 0.0* §	0.3 ± 0.0* §
	Damaged Skin	5.0 ± 1.2* §	0.3 ± 0.1* §	0.4 ± 0.1* §
	Decontaminated Skin	0.4 ± 0.3*	0.02 ± 0.0*	0.1 ± 0.0*
	Broken Skin	398 ± 49	23 ± 2.9	22 ± 2.6
Tritiated stainless steel particles (TSSPs)	Intact Skin	6.8 ± 1.3 ¥ †	0.2 ± 0.1 ¥ †	0.2 ± 0.0 ¥ †
	Damaged Skin	9.9 ± 2.2 ¥ †	0.2 ± 0.0 ¥ †	0.4 ± 0.1 ¥ †
	Decontaminated Skin	1.1 ± 0.6 ¥	0.03 ± 0.01 ¥	0.1 ± 0.0 ¥
	Broken Skin	766 ± 100	17 ± 2.3	19 ± 2.4

Table 3
Total ^3H retained in human skin after exposure to TCPs and TSSPs under different skin conditions: intact; damaged; decontaminated and broken. Data are shown as mean ± SD ($n = 4$). * Statistical differences between intact skin samples and the other skin samples for TCPs; § statistically differences between decontaminated skin samples and the other skin samples for TCPs; ¥ statistically differences between intact skin samples and the other skin samples for TSSPs; † statistically differences between decontaminated skin samples and the other skin samples for TSSPs.

Particles	Sample	Total Skin (%)
Tritiated cement particles (TCPs)	Intact Skin	6.5 ± 4.3
	Damaged Skin	78 ± 22 * §
	Decontaminated Skin	1.5 ± 1.0
	Broken Skin	57 ± 21 * §
Tritiated stainless steel particles (TSSPs)	Intact Skin	4.2 ± 3.0
	Damaged Skin	90 ± 16 ¥ †
	Decontaminated Skin	1.3 ± 0.5
	Broken Skin	46 ± 12 ¥ †

disruption, ^3H may accumulate within epidermal or dermal microdomains without rapid diffusion into the receptor phase. While this cutaneous retention may initially limit systemic exposure, it raises concerns regarding local β-radiation dose and the potential formation of OBT. The persistence of OBT in human tissues, including cartilage and bone, with long biological half-lives (Hisamatsu et al., 1992), and similar retention reported in skin of hairless rats after HTO exposure (Horvath et al., 1992), support the hypothesis that dermally formed OBT could act as a long-term local radiation source. However, OBT formation was not directly measured in the present study, and therefore this hypothesis remains speculative and warrants dedicated investigation. A key finding of this study is the demonstrated efficacy of simple water decontamination in significantly reducing ^3H permeation and retention. In decontaminated skin, ^3H permeation and retention were reduced to 0.06–1.5% of the applied dose, compared to values up to 90% in damaged skin and 18–57% in broken skin, clearly demonstrating that water washing is highly effective in minimizing ^3H absorption and accumulation in the skin (Table 3, Fig. 5). Although not completely eliminating uptake, washing proved to be an effective and accessible intervention. From a broader perspective integrating ^3H species, exposure pathways, and biokinetic behavior, is important to point out that HTO is highly mobile, rapidly equilibrates with body water, and contributes mainly to short-term systemic internal dose (Dolin et al., 2025). In contrast, OBT formed through metabolic incorporation or isotopic exchange, exhibits longer tissue retention and different dosimetric characteristics (Diabate and Strack, 1993; Kim et al., 2013). Particle-associated ^3H, such as that released from TSSPs or TCPs, is initially bound within the solid matrix but may be locally released and permeate across compromised skin barriers, as demonstrated in this study. Once in tissues, a fraction of this ^3H may undergo organic binding, potentially contributing to localized dose and prolonged retention. These considerations indicate that the chemical form of ^3H and the exposure route significantly influence biokinetic behavior and dosimetric impact, highlighting the relevance of dermal exposure alongside inhalation and ingestion in occupational radioprotection frameworks. The current study was not intended to perform a formal human or ecological risk assessment, which requires established regulatory frameworks integrating exposure, biokinetics, dosimetry, and dose–response relationships (International Commission on Radiological Protection (ICRP) and United Nations Scientific Committee on the Effects of Atomic Radiation (UNSCEAR). However, the quantitative permeation and retention data obtained from our study provide relevant input for exposure characterization. The present findings reinforce the clinical and occupational relevance of early and effective dermal decontamination following accidental exposure to tritiated materials. By systematically comparing intact, damaged, abraded, and decontaminated human skin, this study provides a realistic model of occupational exposure and offers critical parameters for risk assessment of tritiated particulate matter. While most European research efforts such as TRANSAT and TITANS have focused on inhalation pathways, findings from this study address a crucial knowledge gap in dermal uptake pathways. The demonstrated influence of skin integrity on ^3H permeation underscores the need to integrate dermal exposure considerations into radioprotection frameworks and material safety assessments. This study also presents several limitations. Although the Franz diffusion cell system provides robust *ex vivo* data, it does not replicate key biological processes such as inflammation, active transport, immune responses, and metabolic activity. These factors may influence ^3H bioavailability and retention *in vivo*. In addition, the formation of OBT and potential downstream biological effects were not directly measured in this work, and therefore no conclusions can be drawn regarding biochemical incorporation or long-term radiobiological consequences. Moreover, only water-based decontamination was investigated, while other chemical or physical decontamination strategies could be explored to further enhance removal efficacy. Emerging *in vitro* technologies, including 3D human skin equivalents and microfluidic "skin-on-chip" models (Sutterby et al., 2020; Risueño et al., 2021), could provide more physiologically relevant platforms for future studies. Further *in vivo* investigations and longer exposure scenarios are also warranted to better characterize chronic dermal exposure, bioaccumulation, OBT formation, and potential radiobiological effects of particle-associated ^3H, thereby improving understanding of the dermal fate of ^3H at the material–bio interface.

5. Conclusion

The current study highlights the human skin as a critical route of internal contamination by ^3H released from TSSPs and TCPs, especially when the barrier integrity is compromised. Experimental results confirmed minimal ^3H permeation through intact skin, underscoring the protective function of the *stratum corneum*. In contrast, ^3H absorption markedly increased, by up to two orders of magnitude in damaged or abraded skin, indicating a tangible occupational risk in nuclear decommissioning environments. The distinct release kinetics observed between TSSPs and TCPs are consistent with their differing

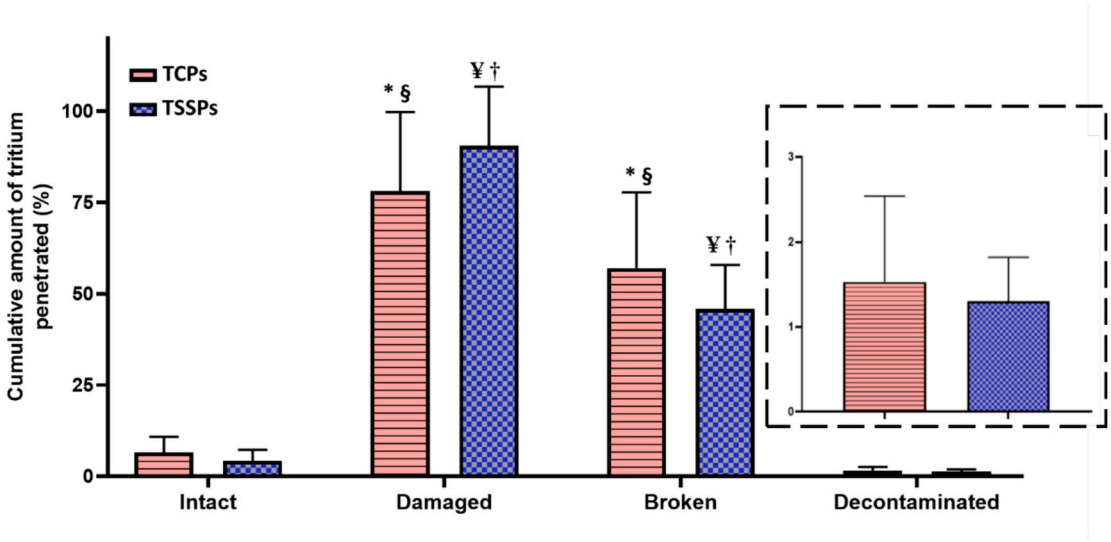

Fig. 5. Amounts of ^{3}H from TSSPs and TCPs that penetrated in the human skin tissue under different conditions: intact; damaged; decontaminated and broken. Data are shown as mean ± SD (n = 4). * statistically differences between intact skin samples and the other skin samples for TCPs; § statistically differences between decontaminated skin samples and the other skin samples for TCPs; ¥ statistically differences between intact skin samples and the other skin samples for TSSPs; † statistically differences between decontaminated skin samples and the other skin samples for TSSPs.

physicochemical behaviors, involving surface adsorption processes. The partial retention of ^{3}H within damaged skin suggests its accumulation in epidermal layers and potential conversion into OBT, raising concerns about localized β-radiation exposure and delayed systemic distribution. Notably, simple decontamination with water significantly reduced both ^{3}H permeation and retention, emphasizing the importance of immediate, accessible radioprotection procedures. Overall, these findings provide novel, quantitative evidence of dermal uptake pathways for tritiated particles, an area scarcely addressed in previous studies and advocate for the inclusion of skin exposure parameters in radiological risk assessments and safety protocols for exposed personnel.

CRediT authorship contribution statement

Greta Camilla Magnano: Writing – review & editing, Writing – original draft, Investigation, Data curation. **Giovanna Marussi:** Investigation. **Matteo Crosera:** Writing – review & editing, Methodology, Formal analysis, Data curation. **Veronique Malard:** Writing – review & editing, Funding acquisition. **Mickael Payet:** Writing – review & editing, Investigation. **Olivier Debellemanière:** Writing – review & editing. **Stefano Covelli:** Writing – review & editing, Supervision. **Daniele Karlicek:** Investigation. **Gianpiero Adami:** Supervision. **Nicola Zingaretti:** Investigation. **Marcella Mauro:** Writing – review & editing. **Elena Pavoni:** Investigation. **Francesca Larese Filon:** Writing – review & editing, Supervision, Funding acquisition, Formal analysis, Conceptualization.

Declaration of competing interest

F. Larese Filon acknowledges funding from the Euratom Research and Innovation Programme under the European Union Framework Programme for Research and Innovation. All other authors declare no competing financial or personal interests that could have influenced the work reported. The views expressed are those of the authors and do not necessarily reflect those of the European Union. This research was conducted as part of the TITANS project, funded by the Euratom Research and Innovation Programme 2022–2025 (Grant Agreement No. 101059408).

Data availability

Data will be made available on request.

Appendix A. Supplementary data

Supplementary data to this article can be found online at https://doi.org/10.1016/j.scitotenv.2026.181735.

References

Austin, J.H., Elleman, T.S., 1972. Tritium diffusion in 304- and 316-stainless steels in the temperature range 25 to 222°C. J. Nucl. Mater. 43 (2), 119–125. https://doi.org/10.1016/0022-3115(72)90145-6.

Bronaugh, Robert L., Stewart, Raymond F., 1985. Methods for in vitro percutaneous absorption studies V: permeation through damaged skin. J. Pharm. Sci. 74 (10), 10. https://doi.org/10.1002/jps.2600741008.

Diabate, Silvia, Strack, Siegfried, 1993. Organically bound tritium. Health Phys. 65 (6), 698–712. https://doi.org/10.1097/00004032-199312000-00008.

Dolin, Viktor, Yakovlev, Yevgenii, Cancemi, Salvatore Angelo, Frano, Rosa Lo, 2025. The impact of tritium in the environment. Appl. Sci. 15 (12), 6664. https://doi.org/10.3390/app15126664.

Eyrolle, Frédérique, Ducros, Loïc, Le Dizès, Séverine, et al., 2018. An updated review on tritium in the environment. J. Environ. Radioact. 181 (janvier), 128–137. https://doi.org/10.1016/j.jenvrad.2017.11.001.

Ferreira, Maria Florencia, Turner, Andrew, Vernon, Emily L., et al., 2023. Tritium: its relevance, sources and impacts on non-human biota. Sci. Total Environ. 876 (juin), 162816. https://doi.org/10.1016/j.scitotenv.2023.162816.

Filon, Larese, Francesca, Giovanna Marussi, Payet, Mickael, et al., 2025. Skin absorption of metals derived from hydrogenated stainless particles in human skin: results from the TITANS project. Environ. Pollut. 364 (janvier), 125327. https://doi.org/10.1016/j.envpol.2024.125327.

Gattu, S., Maibach, H.I., 2010. Enhanced absorption through damaged skin: an overview of the in vitro human model. Skin Pharmacol. Physiol. 23 (4), 171–176. https://doi.org/10.1159/000288163.

Guth, Katharina, Schäfer-Korting, Monika, Fabian, Eric, Landsiedel, Robert, van Ravenzwaay, Ben, 2015. Suitability of skin integrity tests for dermal absorption studies in vitro. Toxicol. In Vitro 29 (1), 1. https://doi.org/10.1016/j.tiv.2014.09.007.

Hisamatsu, S., Katsumata, T., Takizawa, Y., 1992. Tritium concentration in foods and human tissues: estimation of mean residence times of organically-bound tritium in costal cartilage and sternum. J. Radioanal. Nucl. Chem. Artic. 161 (2), 455–463. https://doi.org/10.1007/bf02040492.

Hollenberg, G.W., Simonen, E.P., Kalinin, G., Terlain, A., 1995. Tritium/hydrogen barrier development. Fusion Eng. Des. 28 (mars), 190–208. https://doi.org/10.1016/0920-3796(95)90039-x.

Hopf, N.B., Champmartin, C., Schenk, L., et al., 2020. Reflections on the OECD guidelines for in vitro skin absorption studies. Regul. Toxicol. Pharmacol. 117 (novembre), 104752. https://doi.org/10.1016/j.yrtph.2020.104752.

Horvath, F.J., Légaré, M., Trivedi, A., 1992. Modelling of human and animal data from skin contact exposures to tritium gas contaminated surfaces. Fusion Technol. 21 (2P2), 625–628. https://doi.org/10.13182/fst92-a29817.

IAEA, 1998. Water and Environment News, Issue 3, April 1998: IAEA Subprogram on Water Resources – Tritium Measurements (IAEA/WE/NL/3). avril 3. International Atomic Energy Agency, Vienna.

ISO, 2019. International Organization for Standardization (ISO), 2019. In: ISO 9698: 2019 – Glass: Codification of Glass Surface Features. ISO, Geneva, Switzerland.

Kezic, Sanja, Nielsen, J.B., 2009. Absorption of chemicals through compromised skin. Int. Arch. Occup. Environ. Health 82 (6), 6. https://doi.org/10.1007/s00420-009-0405-x.

Kim, S.B., Baglan, N., Davis, P.A., 2013. Current understanding of organically bound tritium (OBT) in the environment. J. Environ. Radioact. 126 (décembre), 83–91. https://doi.org/10.1016/j.jenvrad.2013.07.011.

Liger, Karine, Grisolia, Christian, Cristescu, Ion, et al., 2018. Overview of the TRANSAT (TRANSversal actions for tritium) project. Fusion Eng. Des. 136 (novembre), 168–172. https://doi.org/10.1016/j.fusengdes.2018.01.037.

Matsumoto, Hideki, Shimada, Yoshiya, Nakamura, Asako J., et al., 2021. Health effects triggered by tritium: how do we get public understanding based on scientifically supported evidence? J. Radiat. Res. 62 (4), 557–563. https://doi.org/10.1093/jrr/rrab029.

Matsuyama, M., Chen, Z., Nisimura, K., et al., 2011. Trapping and depth profile of tritium in surface layers of metallic materials. J. Nucl. Mater. 417 (1–3), 900–903. https://doi.org/10.1016/j.jnucmat.2011.04.005.

OECD, 2004a. Guidance Document for the Conduct of Skin Absorption Studies. OECD, OECD Series on Testing and Assessment. https://doi.org/10.1787/9789264078796-en.

OECD, 2004b. Guideline for the Testing of Chemicals: Skin Absorption: In Vitro Method (N°428).

Ono, Futaba, Tanaka, Satoru, Yamawaki, Michio, 1995. Tritium sorption by cement and subsequent release. Fusion Eng. Des. 28 (mars), 378–385. https://doi.org/10.1016/0920-3796(95)90064-0.

Osborne, R.V., 1966. Absorption of tritiated water vapour by people. Health Phys. 12 (11), 1527–1538. https://doi.org/10.1097/00004032-196611000-00002.

Paquet, F., Bailey, M.R., Leggett, R.W., et al., 2016. ICRP publication 134: occupational intakes of radionuclides: part 2. Ann. ICRP 45 (3–4), 7–349. https://doi.org/10.1177/0146645316670045.

Pinson, Ernest A., Langham, Wright H., 1957. Physiology and toxicology of tritium in man. J. Appl. Physiol. 10 (1), 108–126. https://doi.org/10.1152/jappl.1957.10.1.108.

Risueño, I., Valencia, L., Jorcano, J.L., Velasco, D., 2021. Skin-on-a-chip models: general overview and future perspectives. APL Bioeng. 5, 3. https://doi.org/10.1063/5.0046376.

Smith, Rachel, Ellender, Michele, Guo, Chang, et al., 2022. Biokinetics and internal dosimetry of tritiated steel particles. Toxics 10 (10), 602. https://doi.org/10.3390/toxics10100602.

Sutterby, Emily, Thurgood, Peter, Baratchi, Sara, Khoshmanesh, Khashayar, Pirogova, Elena, 2020. Microfluidic skin-on-a-chip models: toward biomimetic artificial skin. Small 16, 39. https://doi.org/10.1002/smll.202002515.